

Article

Development Progress of 3–5 μm Mid-Infrared Lasers: OPO, Solid-State and Fiber Laser

Tingwei Ren ¹, Chunting Wu ^{1,*}, Yongji Yu ¹, Tongyu Dai ², Fei Chen ³ and Qikun Pan ³

¹ Jilin Key Laboratory of Solid-State Laser Technology and Application, School of Science, Changchun University of Science and Technology, Changchun 130022, China; 2020100071@mails.cust.edu.cn (T.R.); yuyongjiyuyongji@163.com (Y.Y.)

² National Key Laboratory of Tunable Laser Technology, Harbin Institute of Technology, Harbin 150001, China; daitongyu@hit.edu.cn

³ State Key Laboratory of Laser Interaction with Matter, Changchun Institute of Optics, Fine Mechanics and Physics, Chinese Academy of Sciences, Changchun 130033, China; feichenny@126.com (F.C.); panqikun2005@163.com (Q.P.)

* Correspondence: bigsnow1@126.com

Abstract: A 3–5 μm mid-infrared band is a good window for atmospheric transmission. It has the advantages of high contrast and strong penetration under high humidity conditions. Therefore, it has important applications in the fields of laser medicine, laser radar, environmental monitoring, remote sensing, molecular spectroscopy, industrial processing, space communication and photoelectric confrontation. In this paper, the application background of mid-infrared laser is summarized. The ways to realize mid-infrared laser output are described by optical parametric oscillation, mid-infrared solid-state laser doped with different active ions and fiber laser doped with different rare earth ions. The advantages and disadvantages of various mid-infrared lasers are briefly described. The technical approaches, schemes and research status of mid-infrared lasers are introduced.

Keywords: mid-infrared; optical parametric oscillator (OPO); solid-state lasers; fiber lasers



Citation: Ren, T.; Wu, C.; Yu, Y.; Dai, T.; Chen, F.; Pan, Q. Development Progress of 3–5 μm Mid-Infrared Lasers: OPO, Solid-State and Fiber Laser. *Appl. Sci.* **2021**, *11*, 11451. <https://doi.org/10.3390/app112311451>

Academic Editor: Bernhard Wilhelm Roth

Received: 2 November 2021

Accepted: 24 November 2021

Published: 3 December 2021

Publisher's Note: MDPI stays neutral with regard to jurisdictional claims in published maps and institutional affiliations.



Copyright: © 2021 by the authors. Licensee MDPI, Basel, Switzerland. This article is an open access article distributed under the terms and conditions of the Creative Commons Attribution (CC BY) license (<https://creativecommons.org/licenses/by/4.0/>).

1. Introduction

Laser has been an important invention in the history of human science since the 20th century, following atomic energy, semiconductors and computers, known as “the fastest knife”, “the most accurate ruler” and “the brightest light”. Laser has been widely used and recognized in production and science because of its incomparable advantages over ordinary light sources. After 60 years of research and development, laser-related technologies, products and services have spread all over the world, forming a rich and huge laser industry. It is widely used in material processing, communication, optical storage, medical and beauty technologies, research and military developments, instruments and sensors, entertainment display, additive manufacturing and other areas of the national economy. In particular, high-performance 3–5 μm mid-infrared laser in the atmospheric window has important application value and prospect in laser imaging, chemical remote sensing, the medical field, environmental protection and civil and military fields [1].

At present, the technical ways to realize the mid-infrared laser output at a 3–5 μm band mainly include indirect conversion and direct generation. The indirect conversion is mainly based on the nonlinear frequency conversion crystal to generate mid-infrared laser by using an optical parametric oscillator, and the direct generation of stimulated radiation mainly includes quantum lasers, chemical lasers, gas lasers, solid-state lasers and fiber lasers [2]. The characteristic analysis of various ways to realize mid-infrared laser output is shown in Table 1.

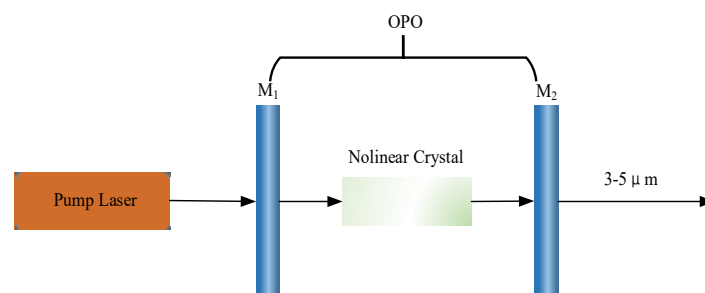
Table 1. Comparative analysis of research approaches for realizing mid-Infrared 3–5 μm band.

Method	Technology	Classification	Advantage	Disadvantage
Indirect conversion	Optical Parametric Oscillator	LiNbO ₃ , PPLN, MgO: PPLN, KTP, KTA, ZnGeP ₂ , AgGaSe ₂ , AgGaS ₂	high energy and efficiency and excellent spectral characteristics	system stability and beam quality should be improved
Directly produced	Quantum Cascade Laser	InAs, AlSb	wider transmission bandwidth	low output power and poor beam quality
	Chemical laser	HF, COIL	good beam quality	high prices, toxic products
	Gas laser	CO, CO ₂	high power and long service life	high temperature explosive, large volume and high cost
	solid-state laser	Fe: ZnSe, Cr: ZnSe	absorption bandwidth, wide tuning range and good beam quality	limited by temperature
	Fiber Laser	Er ³⁺ : ZBLAN, Ho ³⁺ : ZBLAN, Dy ³⁺ : ZBLAN	small transmission loss and stable property	narrow tuning range

As shown in the table, in view of the characteristics of the simple structure, small size, easy application and so on, this paper focuses on the introduction on the research of an optical parametric oscillator, excessive metal doped solid-state lasers and a fiber laser whose gain medium is soft glass.

2. Mid-Infrared Optical Parametric Oscillation Laser (OPO)

The optical parametric oscillation laser (OPO) is one of the main ways to realize a mid-infrared laser output of 3–5 μm and is composed of nonlinear crystal, a pump source and a resonant cavity, as shown in Figure 1. It can reach an output band that cannot be realized by traditional lasers and has many advantages, such as a wide tuning range, simple structure, high output power, narrow linewidth, etc. [3]. With the emergence of various nonlinear crystals, the optical parametric oscillator has achieved important breakthroughs and opened new application prospects, which has once again become a research hot spot of scholars in the world. According to the different nonlinear crystal materials, the mid-infrared laser based on optical parametric oscillation is classified as follows.

**Figure 1.** Schematic diagram of optical parametric oscillator.

2.1. LiNbO₃, PPLN, MgO-Doped PPLN Optical Parametric Oscillator

The optical parametric oscillators of lithium niobate crystals can be divided into pure lithium niobate (LiNbO₃), periodically poled lithium niobate (PPLN) and periodically polarized lithium niobate doped with MgO (MgO-doped PPLN) optical parametric oscillators based on different crystals. The specific evolution process is shown in Figure 2. In order to improve the damage threshold and stability of the crystal, PPLN is used instead of the traditional LiNbO₃ crystal. While in order to further improve the damage threshold of the PPLN crystal, MgO-doped PPLN crystal was born.

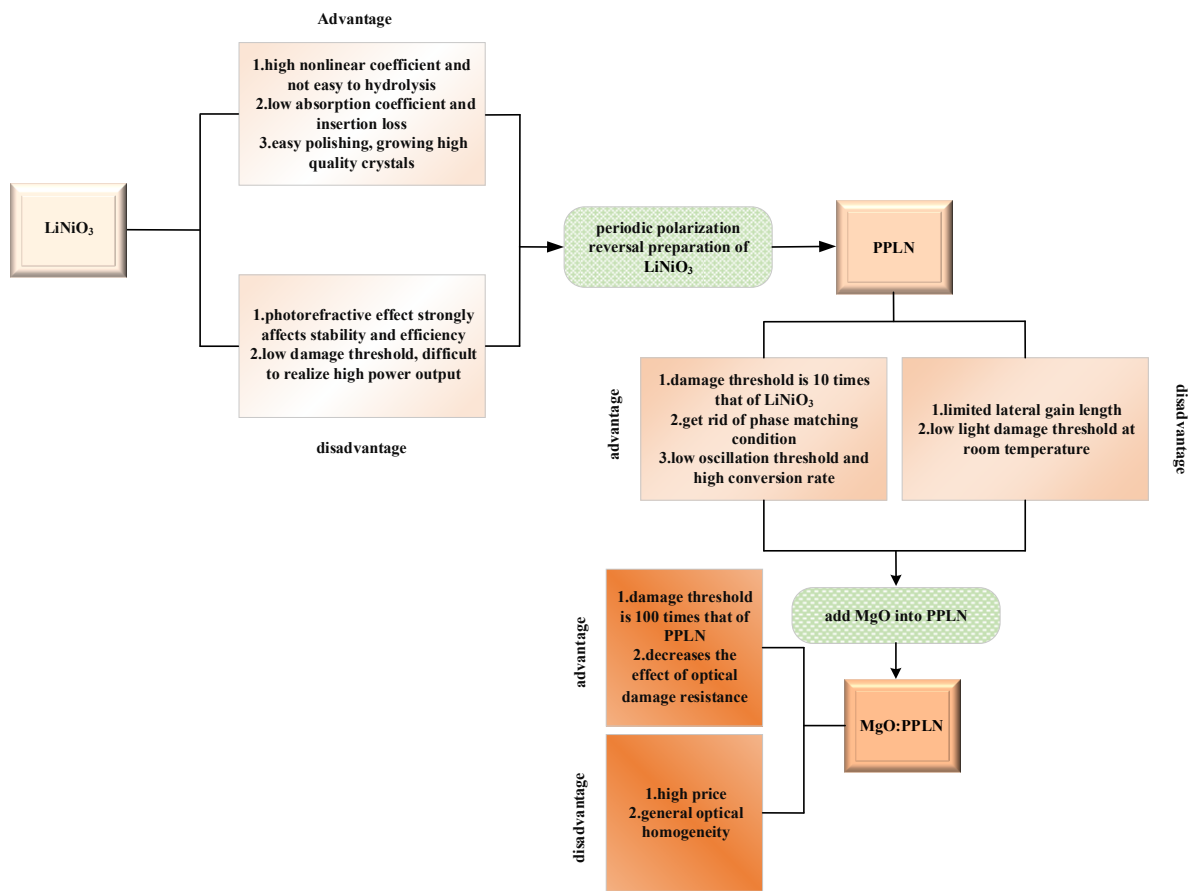


Figure 2. Evolution process of LiNiO₃ crystal.

From Figure 2, we can see that LiNbO₃, PPLN and MgO-doped PPLN all have their own advantages and disadvantages. The technology of periodically polarized crystals has been gradually developed and perfected with the increasing research of scholars. The research statuses of LiNiO₃, PPLN and MgO-doped PPLN optical parametric oscillation lasers are shown in Table 2.

Table 2. Research and development status.

Crystal	Year	Research Establishment	Crystal Parameter	Pump Source	Mid-Infrared Output Parameter	Reference
LiNbO ₃	2000	North China Institute of Optoelectronic Technology	10 × 10 × 30 mm ³	1.06 μm Nd: YAG	Output wavelength 3.76 μm Repetition rate 5 Hz Average power 35 mW Optical efficiency 6%	[4]
	2003	Harbin Institute of Technology	No mention	1.06 μm Nd: YAG	Output wavelength 3.41 μm Repetition rate 10 Hz Average power 12 mW Optical efficiency 4.5%	[5]
	2006	Sichuan University	13 × 13 × 50 mm ³	1.064 μm Nd: YAG	Output wavelength 3.06 μm Repetition rate 1 Hz Average power 15 mW Optical efficiency 10%	[6]
PPLN	2011	Photonics Center	10 × 20 × 0.5 mm ³	1.064 μm Nd: YVO ₄	Output wavelength 4.5 μm Average power 1.1 W Optical efficiency 7.5%	[7]
	2012	Tianjin University	24 × 8 × 1 mm ³	1.064 μm Nd: YVO ₄	Output wavelength 3.66 μm Average power 1.54 W Optical efficiency 7%	[8]

Table 2. Cont.

Crystal	Year	Research Establishment	Crystal Parameter	Pump Source	Mid-Infrared Output Parameter	Reference
	2015	Huazhong Institute of Optoelectronics Technology Barcelona	$40 \times 10 \times 1 \text{ mm}^3$	1.064 μm Nd: GdVO ₄	Output wavelength 3.81 μm Repetition rate 10 kHz Average power 5.4 W Optical efficiency 15.88%	[9]
	2019	Institute of Science and Technology	42 mm length 1 thick	1.064 μm Yb ³⁺ fiber	Output wavelength 3.340 μm Average power 3.5 W Optical efficiency 9.5%	[10]
	2008	Harbin Institute of Technology	$50 \times 8.2 \times 1 \text{ mm}^3$ 5% mol	1.047 μm Nd: YAG	Output wavelength 3.26 μm Repetition rate 10 kHz Average power 0.46 W Optical efficiency 15.3%	[11]
	2008	China Academy of Engineering Physics	No mention 5% mol	1.064 μm Yb ³⁺ fiber	Output wavelength 3.7 μm Average power 3.2 W Optical efficiency 18%	[12]
	2010	Tsinghua University	$5 \times 1 \times 30 \text{ mm}^3$ No mention	1.064 μm Nd: YVO ₄	Output wavelength 3.164 μm Repetition rate 76.8 kHz Average power 4.3 W Optical efficiency 17.1%	[13]
	2012	University of Southampton	$50 \times 2 \times 2 \text{ mm}^3$ No mention	1.064 μm Yb ³⁺ fiber	Output wavelength 3.82 μm Repetition rate 100 kHz Average power 5.5 W Optical efficiency 45%	[14]
	2014	Changchun University of Science and Technology	$50 \times 2 \times 2 \text{ mm}^3$ 5% mol	1.064 μm Nd: GdVO ₄	Output wavelength 3.85 μm Repetition rate 200 kHz Average power 1.82 W Optical efficiency 21.3%	[15]
	2014	Zhejiang University	$50 \times 1 \times 10 \text{ mm}^3$ 5% mol	1.064 μm Yb ³⁺ fiber	Output wavelength 3.99 μm Average power 2.1 W Optical efficiency 5.2%	[16]
MgO-doped PPLN	2016	Université Paris-Saclay	1 length 5% mol	1.55 μm Yb ³⁺ fiber	Output wavelength 3.07 μm Repetition rate 125 kHz Average power 1.25 W Optical efficiency 17.9%	[17]
	2017	Imperial College London	$40 \times 10 \times 1 \text{ mm}^3$ 5% mol	1.065 μm Yb ³⁺ fiber	Output wavelength 3.35 μm Repetition rate 1 MHz Average power 6.2 W Optical efficiency 24.3%	[18]
	2018	Changchun University of Science and Technology	$1 \times 8.6 \times 50 \text{ mm}^3$ 5% mol	1.06 μm Nd: YVO ₄	Output wavelength 3.2 μm Average power 1.72 W Optical efficiency 7.17%	
					Output wavelength 3.5 μm Average power 1.39 W Optical efficiency 5.4%	[19]
					Output wavelength 3.8 μm Average power 1.39 W Optical efficiency 3.1%	
					Output wavelength 4.1 μm Average power 0.72 W Optical efficiency 1.84%	
	2020	Xinjiang Normal University	$40 \times 10 \times 2 \text{ mm}^3$ 5% mol	1.064 μm Nd: YAG	Output wavelength 3.4 μm Repetition rate 50 Hz Average power 1.075 W Optical efficiency 10.2%	[20]
	2020	Shandong University	$25 \times 3 \times 1 \text{ mm}^3$ 5% mol	1.937 μm Tm: YAP	Output wavelength 3.87 μm Repetition rate 6 kHz Average power 1.2 W Optical efficiency 19.4%	[21]

Table 2. Cont.

Crystal	Year	Research Establishment	Crystal Parameter	Pump Source	Mid-Infrared Output Parameter	Reference
	2021	Changchun University of Science and Technology	$30 \times 2 \times 5 \text{ mm}^3$ 5% mol	1.064 μm Yb ³⁺ fiber	Output wavelength 3.8225 μm Repetition rate 1 MHz Average power 2.06 W Optical efficiency 11.38%	[22]
	2021	Shandong University	$10 \times 1 \times 50 \text{ mm}^3$ 5% mol	1.064 μm Yb ³⁺ fiber	Output wavelength 3.4 μm Repetition rate 5 kHz Average power 3.68 W Optical efficiency 37%	[23]

It can be seen from the table that the output power, wavelength and conversion efficiencies of periodically poled crystals have been improved substantially from LiNbO₃ to MgO-doped PPLN.

2.2. *KTiOPO₄* and *KTiOAsO₄* Optical Parametric Oscillator

KTP crystal and KTA crystal belong to the isologue, the symmetrical structure of the 2 m point group, which has high hardness and excellent optical properties. They are nonlinear optical materials widely used in frequency conversions. The descriptions of the two crystals are shown in Figure 3.

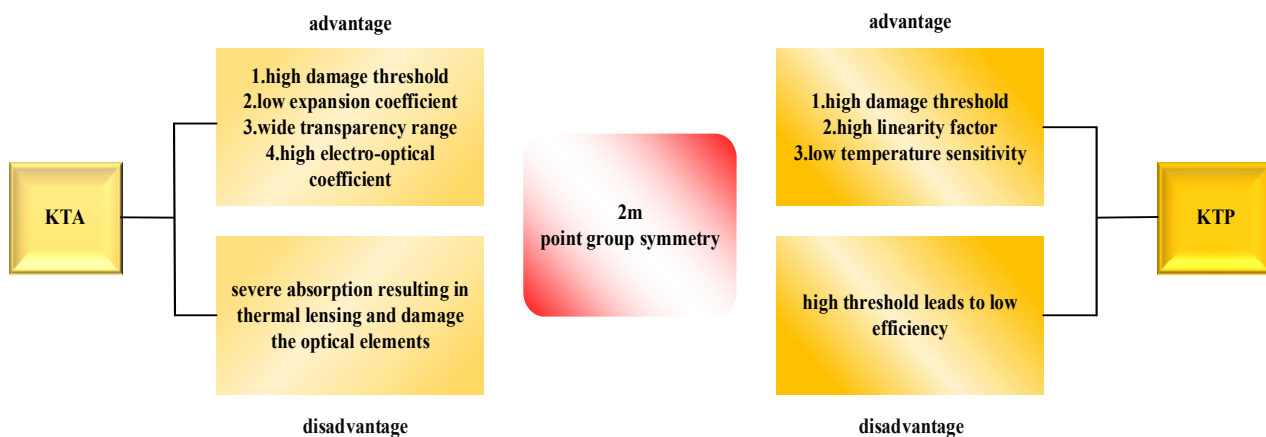


Figure 3. Description diagram of KTP and KTA crystals.

It can be seen from the Figure 3 that both KTP and KTA have the characteristics of a high damage threshold. However, compared with KTP crystal, the physicochemical property of KTA crystal is more stable and overcomes the absorption band of KTP crystal, which is near 3.4 μm . Both crystals have made prominent contributions to the high repetition frequency and high-energy mid-infrared output, and the excellent characteristics of KTP and KTA crystals determine the wide range of their applications. The research progress of KTP and KTA crystals in the mid-infrared band is shown in Table 3.

Numerous institutions for KTP and KTA crystals research have been reported. They have a wide variety of pump sources, and the operation modes are various. According to the latest research, they have achieved high-power and high-quality laser output.

Table 3. Research and development status.

Crystal	Year	Research Establishment	Crystal Parameter	Pump Source	Mid-Infrared Output Parameter	References
KTP	2003	Harbin Institute of Technology	$7 \times 7 \times 25 \text{ mm}^3$	1.06 μm Nd: YAG	Output wavelength 3.29 μm Average power 2 mW Repetition rate 1 Hz Optical efficiency 5%	[5]
	2016	The Czech Academy of Sciences	16.5 mm length 1 mm thickness	0.976 μm Yb ³⁺ fiber	Output wavelength 3.225 μm Repetition rate 100 MHz	[24]
	2018	Humboldt-Universität zu Berlin	2 mm thickness	1.028 μm Yb: KGd(WO ₄) ₂	Output wavelength 3.13 μm Average power 780 mW Repetition rate 100 kHz Optical efficiency 12%	[25]
	2021	Chinese Academy of Sciences	$2 \times 4 \times 4 \text{ mm}^3$	1.03 μm Yb:KGW	Output wavelength 3.17 μm Average power 1.03 W Repetition rate 15 MHz Optical efficiency 14.7%	[26]
KTA	2010	Chinese Academy of Sciences	$5 \times 5 \times 25 \text{ mm}^3$	1.064 μm Nd: YAG	Output wavelength 3.467 μm Average power 84 mW Repetition rate 100 Hz Optical efficiency 14%	[27]
	2011	Norla Institute of Technical Physics	$7 \times 7 \times 20 \text{ mm}^3$	1.064 μm Nd: YAG	Output wavelength 3.475 μm Average power 2.125 W Repetition rate 25 Hz Optical efficiency 14.3%	[28]
	2013	Whenzhou University	$5 \times 5 \times 20 \text{ mm}^3$	0.808 μm Nd: YLF	Output wavelength 3.440 μm Average power 0.335 W Optical efficiency 5.6%	[29]
	2013	Tsinghua University	$10 \times 10 \times 20 \text{ mm}^3$	1.06 μm Nd: YAG	Output wavelength 3.75 μm Average power 600 mW Repetition rate 10 Hz Optical efficiency 7.54%	[30]
	2016	Shanghai Institute of Optics and Fine Mechanics, the Chinese Academy of Sciences	$3 \times 2.5 \times 2 \text{ mm}^3$	0.8 μm Ti: sapphire	Output wavelength 3.27 μm Average power 82 mW Repetition rate 1 kHz Optical efficiency 14.6%	[31]
	2018	Chinese Academy of Sciences	2 mm length	1.03 μm Yb: KGW	Output wavelength 3.05 μm Average power 1.31 W Repetition rate 151 MHz Optical efficiency 18.7%	[32]
	2020	U.S. Army Combat Capabilities Development Command	$6 \times 6 \times 20 \text{ mm}^3$	1.06 μm Nd: YAG	Output wavelength 3.5 μm Average power 0.242 W Repetition rate 20 Hz Optical efficiency 35.5%	[33]
	2021	Shandong University	$10 \times 10 \times 33 \text{ mm}^3$	1.064 μm Nd: YAG	Output wavelength 3.47 μm Average power 6.4 W Repetition rate 100 Hz Optical efficiency 43.6%	[34]

2.3. AgGaSe₂ and AgGaS₂ Optical Parametric Oscillator

AgGaSe₂ and AgGaS₂ are semiconductor chalcopyrite symmetry crystals. Both crystals are transparent in infrared, and they have been used for a long time in the mid-infrared band. The descriptions of two crystals are shown in Figure 4.

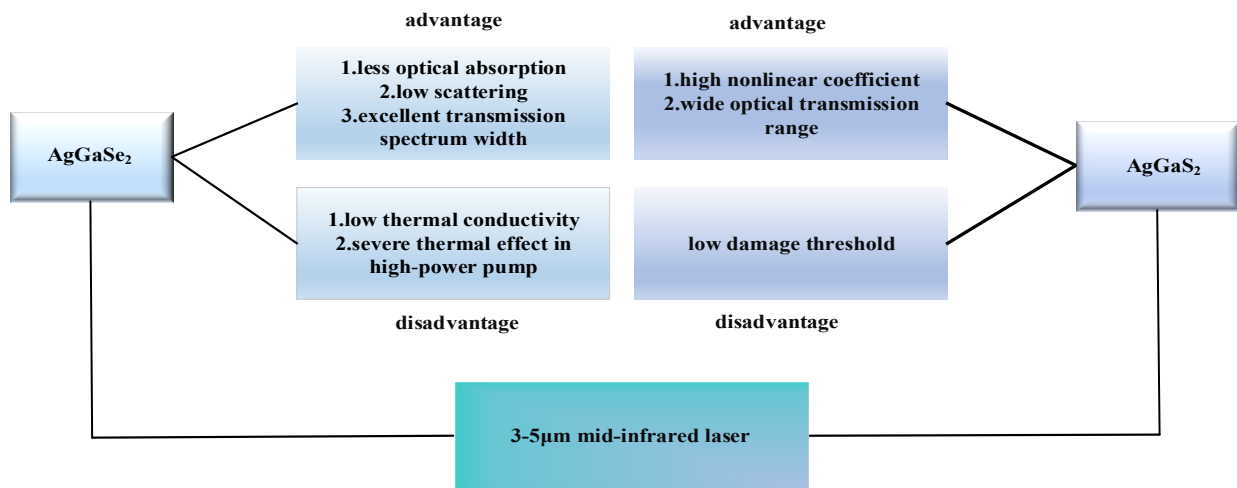


Figure 4. Crystal description diagram.

For AgGaSe₂ and AgGaS₂ crystals, the biggest defect is that the damage interpretation value is generally low, which cannot meet the needs of high repetition rates and maximum energy output.

In the early stage, the research on AgGaSe₂ and AgGaS₂ crystals was also extensive; the research and development status are shown in Table 4.

Table 4. Research and development status.

Crystal	Year	Research Establishment	Crystal Parameter	Pump Source	Mid-Infrared Output Parameter	References
AgGaSe ₂	2000	The University of Burdwan	9 mm thickness	2 µm CO ₂ laser	Output wavelength 3.5 µm Average power 6 mW Repetition rate 1 Hz Optical efficiency 2.4%	[35]
	2009	Changchun Institute of Optics, Fine Mechanics and Physics	18 × 18 × 52 mm ³	9.3 µm TEACO ₂ laser	Output wavelength 4.65 µm Average power 3.9 W Repetition rate 100 Hz Optical efficiency 56%	[36]
	2013	Huazhong University of Science and Technology	5 × 5 × 13 mm ³	9.6 µm CO ₂ laser	Output wavelength 3.2 µm Average power 4 kW Repetition rate 1 Hz Optical efficiency 0.14%	[37]
AgGaS ₂	1984	Stanford University	2 × 1 × 0.5 mm ³	1.064 µm Nd: yttrium	Output wavelength 4 µm Average power 5 mW Repetition rate 10 Hz Optical efficiency 16%	[38]
	1997	DSO National Laboratories	2 × 0.7 × 0.7 mm ³	1.064 µm Nd: YAG	Output wavelength 4.2 µm Repetition rate 10 Hz Optical efficiency 10%	[39]
	1999	American Institute of Physics	20 × 7 × 10 mm ³	1.06 µm Nd: YAG	Output wavelength 3.9 µm Average power 4 mW Repetition rate 10 Hz Optical efficiency 22%	[40]
	2006	Jilin University	10 × 7 × 20 mm ³	1.06 µm Nd: YAG	Output wavelength 4 µm Average power 12 mW Repetition rate 20 Hz Optical efficiency 3.5%	[41]

It can be seen from the existing reports that the output efficiency based on these two crystals to realize mid-infrared laser is low, and the maximum energy that can be obtained

is also relatively small. This may be the reason why there are almost no literature reports about realizing mid-infrared laser output based on these two nonlinear crystals in the past decade.

2.4. ZnGeP_2 Optical Parametric Oscillator

ZnGeP_2 crystal is the most important nonlinear crystal in optical parametric oscillator technology. The description of it is shown in Figure 5.

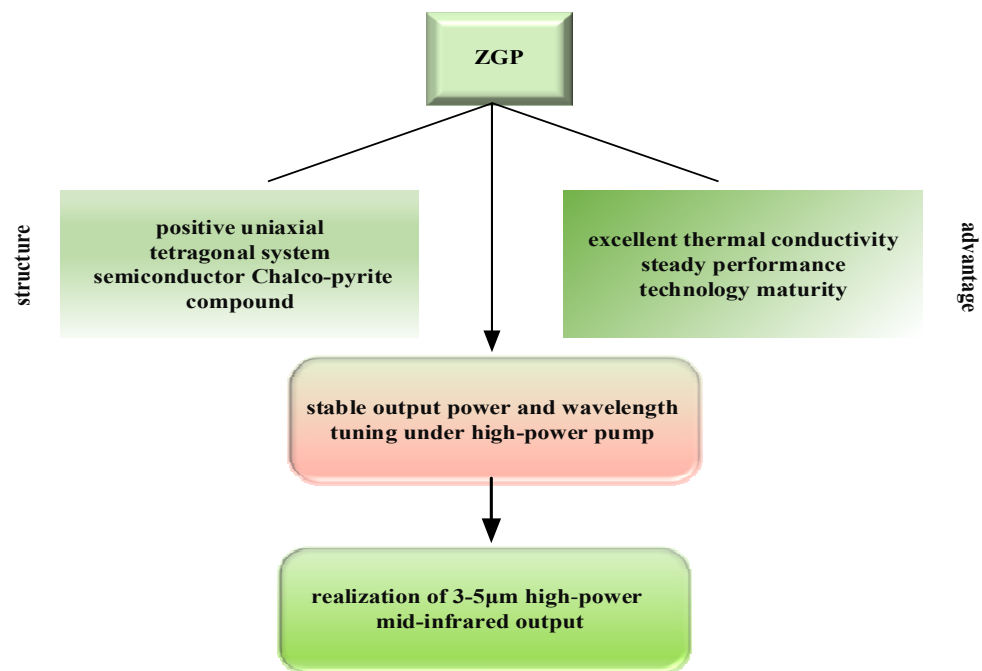


Figure 5. Description diagram of ZGP crystal.

For the ZnGeP_2 crystal, its good physical and chemical properties, high thermal conductivity and damage threshold have achieved its advantages when operating in a high-power environment. Therefore, it is the best nonlinear crystal for a high-power, 3~5 μm mid-infrared OPO.

The ZnGeP_2 crystal has been deeply studied by many scholars because of its excellent characteristics. The research development is shown in Table 5.

According to the literature, the best results of mid-infrared laser output based on ZGP crystal are an average output power of 103 W at a frequency of 10 kHz. The optical efficiencies are 78% and 44.2% with an output wavelength of 4.6 μm and 4.57 μm , respectively.

As mentioned above, several optical parametric oscillators for mid-infrared (3–5 μm) output are discussed. The properties parameters of mid-infrared nonlinear optical crystals are shown in Table 6.

The nonlinear crystals mentioned above have transmittance in the mid-infrared of 3–5 μm , which are currently widely studied in the world. Compared with LiNiO_3 and PPLN, MgO-doped PPLN crystal owns a larger damage threshold, and now it has become a research hotspot. However, the thermal conductivity of KTP, AgGaSe_2 and AgGaS_2 are relatively small, which will induce serious thermal effect under high-power operation and even cause the damage of crystals. Therefore, the output and applications of high-power mid-infrared in the future are limited. The thermal conductivity is smallest, and the damage threshold is the highest of ZGP crystal, which may be the reason why the output power is largest among these nonlinear crystals. It has a compact laser structure, the advantages of a wide tuning range of output wavelength and so on. Therefore, it can be said that the realization of mid-infrared laser output based on ZGP crystal is mainstream through an indirect way.

Table 5. Research and development status.

Year	Research Establishment	ZGP Crystal Parameter	Pump Source	Mid-Infrared Output Parameter	References
2010	Norwegian Defence Research Establishment	$8.5 \times 6 \times 8 \text{ mm}^3$	2.1 μm Ho: YAG	Output wavelength 4.5 μm Average power 22 W Repetition rate 45 kHz Optical efficiency 58%	[42]
2011	China Academy of Engineering Physics	$8 \times 6 \times 18 \text{ mm}^3$	2.1 μm KTP OPO	Output wavelength 4.32 μm Average power 5.7 W Repetition rate 8 kHz Optical efficiency 46.6%	[43]
2013	Australian National University	No mention	2.09 μm Ho: YAG	Output wavelength 3.5 μm Average power 10.6 W Repetition rate 35 kHz Optical efficiency 69%	[44]
2014	University of Central Florida	$5 \times 4 \times 12 \text{ mm}^3$	1.98 μm Tm: fiber	Output wavelength 3.7 μm Average power 2.8 W Repetition rate 4 kHz Optical efficiency 8%	[45]
2014	Harbin Institute of Technology	$6 \times 6 \times 23 \text{ mm}^3$	2.1 μm Ho: YAG	Output wavelength 4.5 μm Average power 41.2 W Repetition rate 20 kHz Optical efficiency 38.5%	[46]
2015	Huabei Photoelectric Technology Research Institute	$5 \times 5 \text{ mm}^2$ end face	2.05 μm Ho: YLF	Output wavelength 3.75 μm Average power 26.9 W Repetition rate 5 kHz Optical efficiency 50%	[47]
2016	French-German Research Institute of Saint-Louis	$14 \times 12 \times 6 \text{ mm}^3$	2.05 μm Ho: YLF	Output wavelength 4.6 μm Average power 0.12 W Repetition rate 1 Hz Optical efficiency 78%	[48]
2017	Chinese Academy of Sciences	$6 \times 6 \times 15 \text{ mm}^3$	2.09 μm Ho: YAG	Output wavelength 4.6 μm Average power 95 mW Repetition rate 5 Hz Optical efficiency 75.7%	[49]
2018	Harbin Institute of Technology	30 mm length	2.05 μm Ho: GdVO ₄	Output wavelength 4.39 μm Average power 2.05 W Repetition rate 5 kHz Optical efficiency 74.6%	[50]
2019	Harbin Institute of Technology	$6 \times 6 \times 20 \text{ mm}^3$	2.09 μm Ho: YAG	Output wavelength 4.57 μm Average power 103 W Repetition rate 10 kHz Optical efficiency 44.2%	[51]
2019	Changchun University of Science and Technology	$5 \times 5 \times 16 \text{ mm}^3$	2.09 μm Ho: YAG	Output wavelength 4.5 μm Average power 5.97 W Repetition rate 6 kHz Optical efficiency 44.1%	[52]
2021	French-German Research Institute of Saint-Louis	$6 \times 6 \times 20 \text{ mm}^3$	2.09 μm Ho:LLF MOPA	Output wavelength 3–5 μm Average power 38 W Repetition rate 10 kHz Optical efficiency 46.6%	[53]
2021	Shandong University	$6 \times 6 \times 25 \text{ mm}^3$	2.1 μm Ho:YAG	Output wavelength 4.3 μm Average power 10.62 W Repetition rate 15 kHz Optical efficiency 37.9%	[54]

Table 6. Properties of mid-infrared nonlinear crystals mentioned above.

Crystal	Crystal System	Point Group	Nonlinear Coefficient/ $\text{pm} \cdot \text{V}^{-1}$	Transparency Range/ μm	Thermal Conductivity/ $\text{W} \cdot \text{m}^{-1} \cdot \text{K}^{-1}$	Damage Threshold/ $\text{GW} \cdot \text{cm}^2$
LiNiO ₃	trigonal system	3 m	$d_{22} = 2.1$ $d_{31} = 4.3$ $d_{33} = 27.2$	0.35–4.5	5.6	0.2
PPLN	trigonal system	3 m	$d_{33} = 27.2$	0.33–5.5	5	0.3
MgO: PPLN	trigonal system	3 m	$d_{13} = 14.8$	0.36–5	4.4	0.6
KTP	orthorhombic system	2 m	$d_{15} = 1.9$ $d_{24} = 3.64$ $d_{33} = 16.9$	0.35–4.5	0.4	1.5
KTA	orthorhombic system	2 m	$d_{15} = 4.2$ $d_{24} = 2.8$ $d_{33} = 16.2$	0.4–5	20	1.0
AgGaSe ₂	tetragonal system	42 m	$d_{36} = 39.5$	0.73–18	1	0.04
AgGaS ₂	tetragonal system	42 m	$d_{36} = 13.4$	0.53–13	1.5	0.04
ZGP	tetragonal system	42 m	$d_{\text{eff}} = 75$	0.74–12	35	30

3. Mid-Infrared Fe: ZnSe and Cr: ZnSe Solid-State Lasers

Taking transition metal doped II~VI chalcogenides crystallized group sulfide crystals as gain media is an important means to realize mid-infrared laser. The two typical laser materials are Fe: ZnSe and Cr: ZnSe crystals. Characteristics descriptions of Fe: ZnSe and Cr: ZnSe crystals are shown in Figure 6.

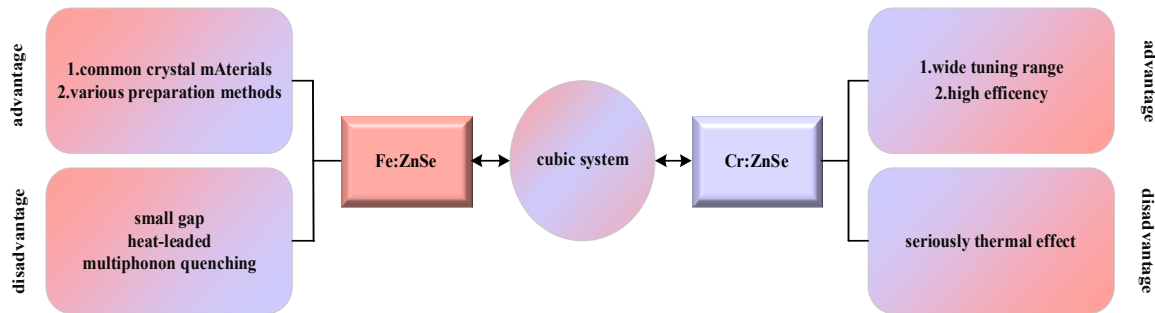


Figure 6. Characteristics descriptions of Fe: ZnSe and Cr: ZnSe crystals.

Fe: ZnSe is a four-energy level structure. When Fe²⁺ is doped into ZnSe, Zn²⁺ in the center of tetrahedron will be replaced. The ground state energy level ⁵D of the outermost electron ³d₆ splits into duplex degenerate states ⁵E and triple-degenerate states ⁵T₂ under the action of a crystal field [55]. Then the one-step orbital spin coupling splits the ⁵T₂ state into three energy bands and the second-order orbital spin coupling splits the ⁵E state into five energy levels. The energy level diagram is shown as Figure 7.

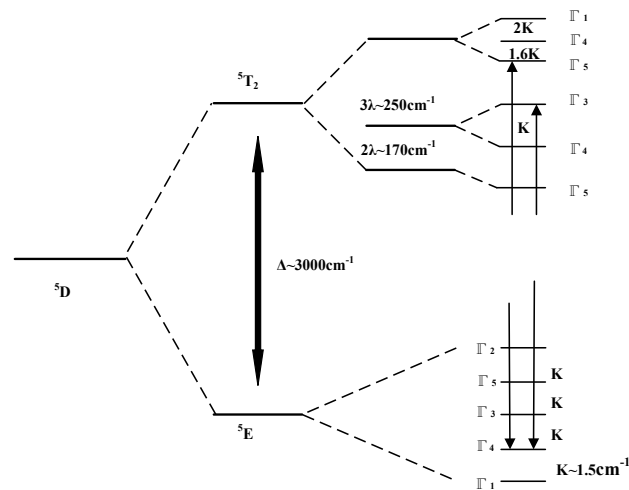


Figure 7. Diagram of Fe: ZnSe energy level.

Cr: ZnSe is a four-energy level structure. Under the action of a pump light, Cr^{2+} in the ground state of ${}^5\text{T}_2$ transits to the vibrational levels of excited state ${}^5\text{E}$, and because there is no other energy level above the ${}^5\text{E}$ excited state level, therefore, there is almost no excited state absorption process for Cr^{2+} [56]. The energy level diagram is shown as Figure 8.

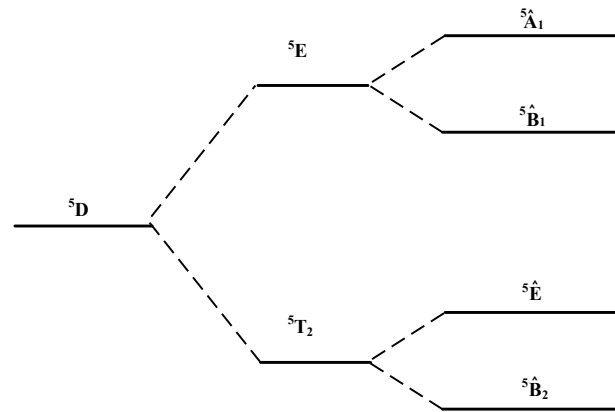


Figure 8. Diagram of Cr: ZnSe energy level.

The absorption peak of Fe: ZnSe crystal is near $3\ \mu\text{m}$ at room temperature. Additionally, the emission peak is near $4.3\ \mu\text{m}$. Take note that the absorption characteristics of Fe: ZnSe crystal varies greatly with temperature, as shown in Figure 9. The absorption cross sections of Fe: ZnSe crystal are greatly at 14 K. Additionally, the absorption cross section will become lower while, at the same time, the absorption range will become wider at 300 K. From the emission spectrum of Fe: ZnSe, the material emission spectrum range is $3\text{--}5\ \mu\text{m}$ [1].

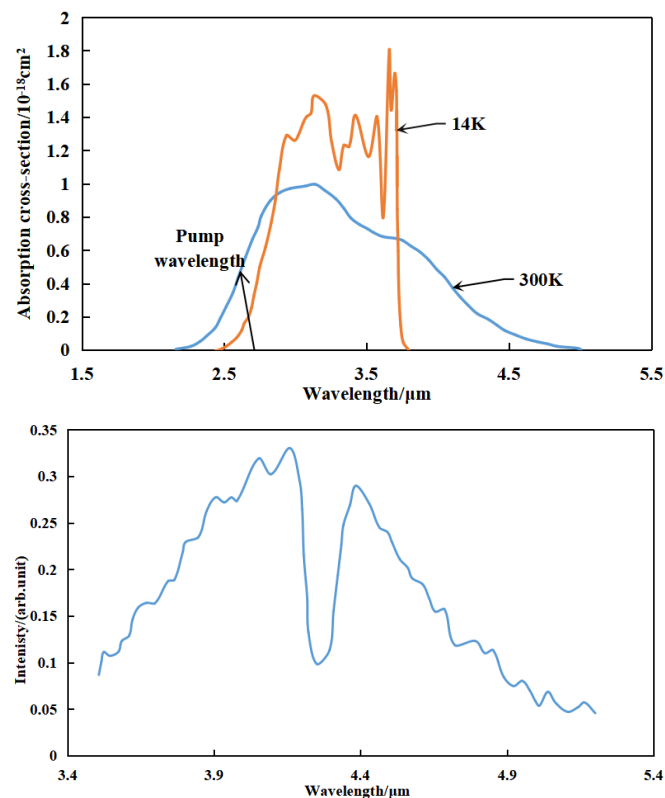


Figure 9. Absorption and emission spectrum of Fe: ZnSe crystal.

Cr: ZnSe has a relatively wide absorption band, at 1.5–2 μm ; as shown in Figure 10, the absorption peak is around 1.75 μm . The emission spectroscopy is 2–3 μm , and the emission peak is about 2.45 μm [56]. It can be seen from Figure 10 that it is not a good choice to use the Cr: ZnSe crystal to achieve a laser output above 3 μm , because, although the crystal has emission at 3 μm , its gain is relatively low.

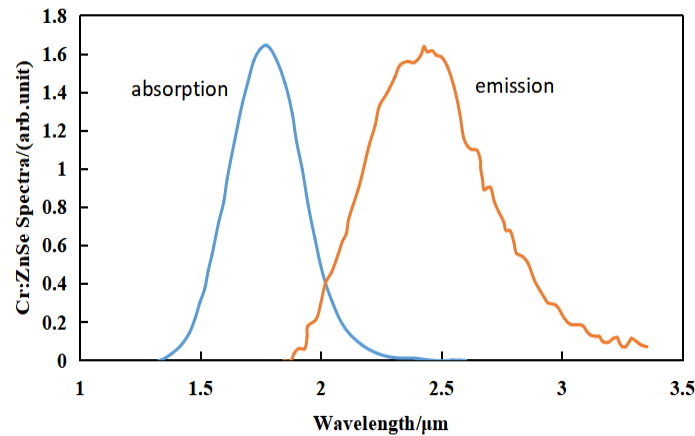


Figure 10. Absorption and emission spectrum of Cr: ZnSe crystal.

Spectroscopic and material properties of the Cr: ZnSe and Fe: ZnSe crystals are shown in Table 7.

Table 7. Parameters of Cr: ZnSe and Fe: ZnSe crystals.

Crystal	Cr:ZnSe	Fe:ZnSe
Symmetry of crystal	Cubic system	Cubic system
Size (mm^3)	$40 \times 40 \times 50$	$40 \times 40 \times 50$
Launch range (μm)	1.9–3.3	3.4–5.2
Gain bandwidth (nm)	500	500
Peak absorption cross section ($\times 10^{-20} \text{ cm}^2$)	87	97
Peak absorption wavelength (μm)	1.78	3 (300 K)
Peak emission cross section ($\times 10^{-20} \text{ cm}^2$)	90	140
Peak emission wavelength (μm)	2.45	4.140
Emission bandwidth (nm)	0.9	1.1
Fluorescence lifetime (300 k, μs)	8	0.37

It can be seen from Table 7 that the absorption cross section and emission cross section of Fe^{2+} : ZnSe are larger than that of Cr^{2+} : ZnSe. While the Cr: ZnSe crystal exhibits excellent room temperature fluorescence properties, both of them have a wide tuning range and high quantum efficiency, which have attracted more and more attention in the field of mid-infrared wave band research. The research and development status of Cr: ZnSe and Fe: ZnSe lasers are shown in Table 8.

Compared with Cr: ZnSe laser, the single energy or the average power is higher for the Fe: ZnSe laser. However, for the Fe: ZnSe crystal, the temperature is the key factor affecting its fluorescence lifetime. High-power Fe: ZnSe laser can be realized at low temperatures. As temperature rises, the fluorescence lifetime of Fe: ZnSe crystal decreases, which makes it difficult to achieve a high-power, mid-infrared laser. Future research can focus on the external cooling method of the laser to ensure that it maintains good mid-infrared laser output performance at room temperature.

Table 8. Research and development status.

Crystal	Year	Research Establishment	Crystal Parameter	Pump Source	Mid-Infrared Output Parameter	References
Fe:ZnSe	2011	University of Alabama at Birmingham	$8 \times 8 \times 3 \text{ mm}^3$ $2 \times 10^{19} \text{ cm}^{-3}$	2.8 μm Er, Cr: YSGG	Temperature 300 k (0.38 μs) Output wavelength 4.3 μm Average power 0.3 mW Optical efficiency 16%	[57]
	2012	Air Force Research Laboratory	$2 \times 6 \times 8 \text{ mm}^3$ $9 \times 10^{18} \text{ cm}^{-3}$	2.94 μm Er: YAG	Temperature 236 k (0.274 μs) Output wavelength 4.37 μm Average power 24.12 mW Optical efficiency 19%	[58]
	2013	Russian Academy of Sciences	$8 \times 8 \times 8 \text{ mm}^3$ $2.6 \times 10^{18} \text{ cm}^{-3}$	2.9 μm Er: YAG	Temperature 300 k (0.37 μs) Output wavelength 4.14 μm Average power 840 mW Optical efficiency 39%	[59]
	2015	Heriot-Watt University	$1.82 \times 4.76 \times 6.94 \text{ mm}^3$ $8.8 \times 10^{18} \text{ cm}^{-3}$	2.94 μm Er: YAG	Temperature 245 k (1.7 μs) Output wavelength 4.5 μm Average power 2.1 W Optical efficiency 23%	[60]
	2015	University of Alabama	2 mm thickness	2.94 μm Er: YAG	Temperature 275 k (0.715 μs) Temperature 292 k (0.36 μs) Temperature 77 K (0.57 μs) Output wavelength 4.122 μm Average power 76 mW Optical efficiency 11%	[61]
	2017	All-Russian Research Institute of Experimental Physics	$120 \times 64 \times 4 \text{ mm}^3$ $(7-9) \times 10^{18} \text{ cm}^{-3}$	2.6 μm HF	Temperature 300 k (0.36 μs) Output wavelength 4.3 μm Average power 20 W	[62]
	2018	Russian Academy of Sciences	$25 \times 25 \times 16.7 \text{ mm}^3$ $1.1 \times 10^{18} \text{ cm}^{-3}$	2.94 μm Er: YAG	Temperature 80 k (60 μs) Temperature 220 k (8 μs) Temperature 250 k (3 μs) Temperature 300 k (0.37 μs) Output wavelength 4.3 μm Average power 7.5 W Optical efficiency 30%	[63]
	2019	Russian Academy of Sciences	12 Diameter \times 17 thickness mm^3 $1.8 \times 10^{18} \text{ cm}^{-3}$	2.94 μm Er: YAG	Temperature 5–18 $^{\circ}\text{C}$ (0.68–0.39 μs) Output wavelength 4.7 μm Average power 3.14 W Optical efficiency 17.5%	[64]
	2019	Harbin Institute of Technology	$4 \times 4 \times 10 \text{ mm}^3$ $5 \times 10^{18} \text{ cm}^{-3}$	2.958 μm Ho, Pr: LLF	Temperature 77 k (0.57 μs) Output wavelength 3.957 μm Average power 0.0164 mW Optical efficiency 22.9%	[65]
	2019	Harbin Institute of Technology	$4 \times 10 \times 10 \text{ mm}^3$ $5 \times 10^{18} \text{ cm}^{-3}$	2.93 μm Cr, Er: YAG	Temperature 77 k (57 μs) Output wavelength 4.037 μm Average power 197.6 mW Optical efficiency 13.7%	[66]
2020	Osaka University	8 length $3.5 \times 10^{18} \text{ cm}^{-3}$	2.8 μm Er: ZBLAN	Temperature 300 k (0.37 μs) Output wavelength 4.509 μm Average power 3.5 mW Optical efficiency 0.27%	[67]	

Table 8. Cont.

Crystal	Year	Research Establishment	Crystal Parameter	Pump Source	Mid-Infrared Output Parameter	References
Cr: ZnSe	2020	Lomonosov Moscow State University	8 length $3.5 \times 10^{18} \text{ cm}^{-3}$	2.8 μm Er: ZBLAN	Temperature 170 k Output wavelength 4.4 μm Average power 415 mW Optical efficiency 5.92%	[68]
	2020	Changchun Institute of Optics, Fine Mechanics and Physics	28 mm diameter 4 mm thickness $2 \times 10^{18} \text{ cm}^{-3}$	2.6 μm HF	Temperature 300 k (0.37 μs) Output wavelength 3.1 μm Average power 21.7 W Optical efficiency 32.6%	[69]
	2021	University of Alabama at Birmingham	2–3 mm length $1.5 \times 10^{19} \text{ cm}^{-3}$	2.94 μm Er: YAG	Temperature 120 k (57 μs) Temperature 300 k (0.37 μs) Output wavelength 4.1 μm Average power 180 mW Optical efficiency 25%	[70]
	2006	Koç University	2 mm thickness $5.7 \times 10^{18} \text{ cm}^{-3}$	1.57 μm KTP OPO	Temperature 300 k (5 μs) Output wavelength 3.1 μm Average power 145 mW Optical efficiency 8%	[71]
	2007	University of Alabama at Birmingham	$4 \times 8 \times 1 \text{ mm}^3$ No mention	1.55 μm Er ³⁺ fiber	Output wavelength 3 μm Average power 150 mW	[72]
	2010	Norwegian University of Science and Technology	2.3 thickness mm $5 \times 10^{18} \text{ cm}^{-3}$	1.607 μm Er ³⁺ fiber	Output wavelength 3.3 μm Average power 600 mW	[73]
	2021	Tokyo University of Science	5 length mm $8 \times 10^{-18} \text{ cm}^{-3}$	2.01 μm Tm:YAG	Output wavelength 3.2 μm Average power 49.8 mW Optical efficiency 22.5%	[74]

4. Mid-Infrared Fiber Lasers

Optical fiber has many advantages in numerous fields. This paper mainly discusses the mid-infrared fiber laser with soft glass [fluoride (Er³⁺, Ho³⁺, Dy³⁺), chalcogenide, telluride] as the gain medium. The description is shown in Figure 11.

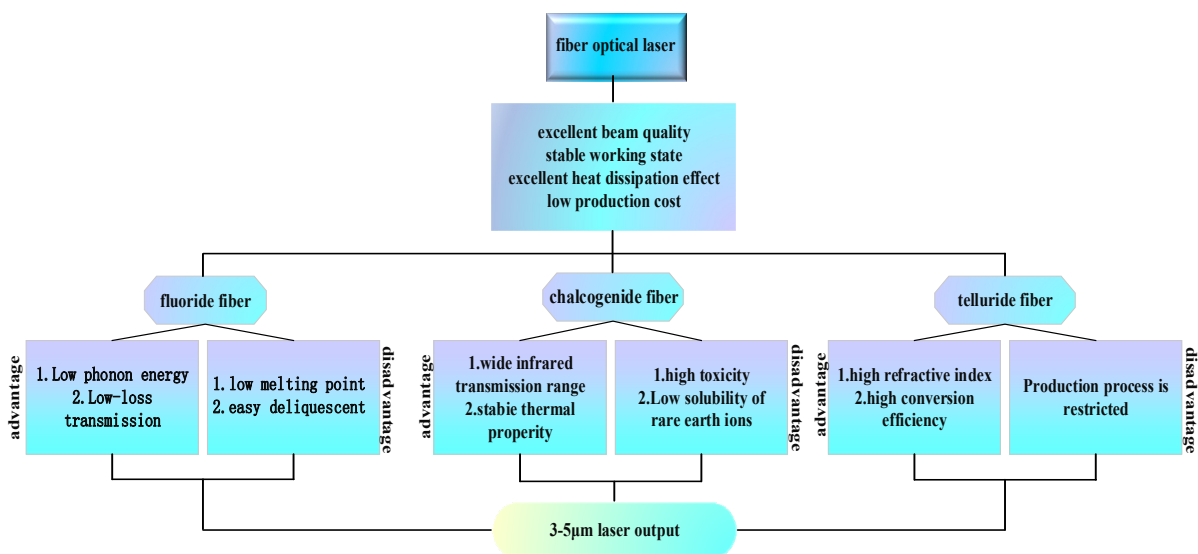


Figure 11. Description diagram of mid-infrared fiber lasers.

The most-used material for fluoride optical fiber is a multi-component fluoride glass called “ZBLAN”; the mid-infrared fiber laser operating at 3–5 μm band has a similar outer electron arrangement for gain ions. Energy level transitions between configurations produce abundant emission lines; the gain fiber mainly includes Er³⁺, Ho³⁺, Dy³⁺, and its energy level diagram [75] is shown in Figure 12.

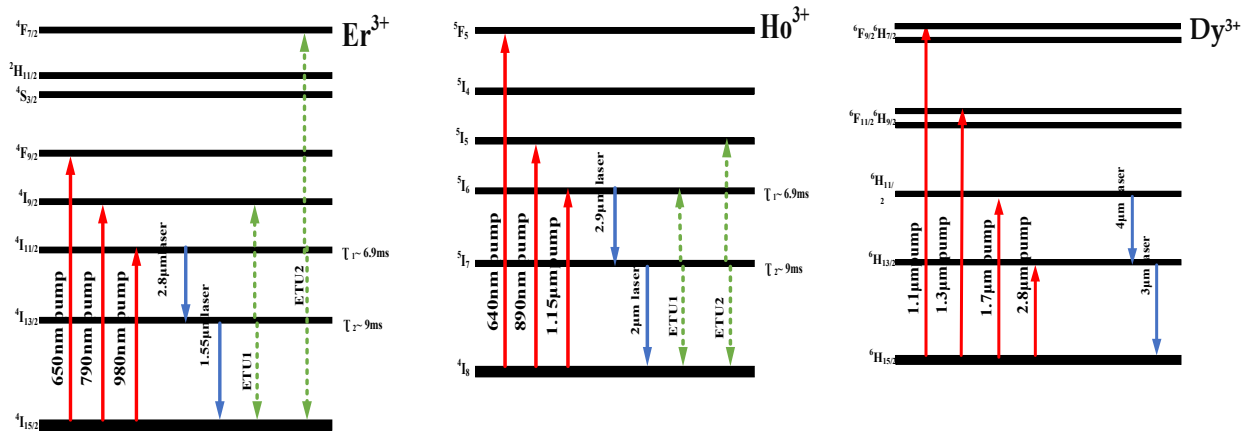


Figure 12. Energy level diagram.

The chalcogenide glass has excellent mid-infrared transmission, thermal and mechanical properties. Compared with fluoride glass fiber, its phonon energy is lower, which makes up for the defect that ZBLAN is hindered to work at wavelengths exceeding 4 μm due to the reduction of high-energy states caused by multi-phonon transitions. In the context of the chalcogenide glass fiber lasers, the ions that have received the most attention are praseodymium and terbium. The energy level diagram [76] is shown in Figure 13.

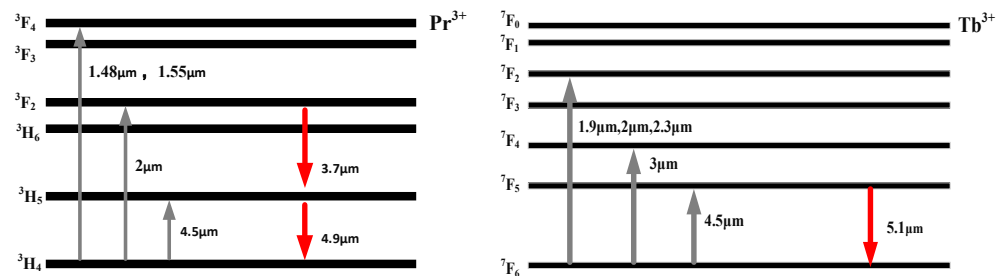


Figure 13. Energy level diagram.

For the glass fibers of fluoride, chalcogenide and tellurite, their physical and chemical properties are different, as shown in Table 9.

Table 9. Physicochemical properties of various soft glass fibers.

Properties	Fluoride	Chalcogenide	Tellurite
The lowest loss (dB/m)	0.45×10^{-3}	0.023	0.02
Max. phonon energy (cm ⁻¹)	560	300–450	700
Transparency (μm)	0.4–6	1–16	0.5–5
Nonlinear refractive index (×10 ⁻²⁰ m ² /W)	2–3	300–500	59
Melting point (°C)	265	250	500
Durability	poor	good	good
Toxicity	high	high	safe

Compared with chalcogenides, the fluoride glass has lower loss but higher phonon energy, and its transparency range is far inferior to chalcogenide's. However, compared with tellurite glass, the fluoride glass and chalcogenide glass are more toxic. Three kinds of glass optical fibers are the best choice for mid-infrared transmission. Their low optical loss and high-power damage threshold make many applications possible.

The fiber lasers with different gain media have unique advantages and characteristics. The developments are shown in Table 10.

Table 10. Research and development status.

Medium	Fiber Matrix	Year	Research Establishment	Crystal Parameter	Pump Source	Mid-Infrared Output Parameter	References		
Fluoride	Er: ZBLAN	2014	The University of Adelaide	18 mm length 1 %mol	1.973 μm fiber laser	Output wavelength 3.5 μm Average power 260 mW Optical efficiency 16%	[77]		
		2016	Chinese Academy of Sciences	0.9 mm length 6% mol	0.975 μm LD pump beam	Output wavelength 3 μm Average power 1.01 W Repetition rate 146.3 kHz Optical efficiency 17.8%	[78]		
		2018	Shanghai Jiao Tong University	2.8 mm length 1% mol	1.973 μm Tm ³⁺ fiber	Output wavelength 3.489 μm Average power 40 mW Repetition rate 28.91 MHz Optical efficiency 18%	[79]		
		2019	Université Laval	2.5 mm length 7% mol	976 + 1976 nm LD pump beam	Output wavelength 3.42 μm Average power 3.4 W Optical efficiency 38.6%	[80]		
		2020	University of Electronic Science and Technology of China	3.2 mm length 1.5% mol	976 + 1981 nm LD pump beam	Output wavelength 3.45 μm Average power 264.5 mW Optical efficiency 7.18%	[81]		
		2021	Shenzhen University	1.8 mm length 1% mol	976 + 1973 nm LD pump beam	Output wavelength 3.46 μm Average power 63 mW Repetition rate 58.71 MHz Optical efficiency 15.6%	[82]		
	Ho: ZBLAN	Ho: ZBLAN	2011	University of Sydney	10 mm length 1.2% mol	1.15 μm LD pump beam	Output wavelength 3.002 μm Average power 77 mW Optical efficiency 12.4%	[83]	
			2012	University of Electronic Science and Technology of China	12 mm length 1.2% mol	1.15 μm LD pump beam	Output wavelength 3.005 μm Average power 175 mW Repetition rate 75 kHz	[84]	
			2013	University of Arizona	2.5 mm length 3% mol	1.15 μm Roman laser	Output wavelength 3 μm Average power 100 mW Repetition rate 100 kHz Optical efficiency 12.3%	[85]	
		Ho:InF ₃	2018	Université Laval	2.3 mm length 10% mol	888 nm LD pump beam	Output wavelength 3.92 μm Average power 197 mW Optical efficiency 9.77%	[86]	
			2021	University of Electronic Science and Technology of China	0.23 mm length 10% mol	888 + 974 nm LD pump beam	Output wavelength 3.92 μm Average power 1.3 W Optical efficiency 21.6%	[87]	
			2016	Macquarie University	0.92 mm length 2000 ppm	2.8 μm Er: ZBLAN	Output wavelength 3.04 μm Average power 80 mW Optical efficiency 51%	[88]	
			2016	Macquarie University	0.14 mm length 2000 ppm	2.8 μm Er: ZBLAN	Output wavelength 3.26 μm Average power 120 mW Optical efficiency 37%	[88]	
			Dy: ZBLAN	2018	Macquarie University	0.6 mm length 2000 ppm	1.7 μm Raman laser	Output wavelength 3.4 μm Average power 170 mW Optical efficiency 21%	[89]
				2019	Université Laval	2.2 mm length 2000 ppm	2.83 μm Er: ZBLAN	Output wavelength 3.24 μm Average power 10.1 W Optical efficiency 58%	[90]

Table 10. Cont.

Medium	Fiber Matrix	Year	Research Establishment	Crystal Parameter	Pump Source	Mid-Infrared Output Parameter	References
		2020	Université Laval	1.75 mm length 2000 ppm	2.825 μm Er: ZBLAN	Output wavelength 3.24 μm Average power 1.43 W Repetition rate 120 kHz Optical efficiency 22%	[91]
	Dy:InF ₃	2021	University of Electronic Science and Technology of China	1.25 mm length 0.1% mol	1.1 μm Yb ³⁺ :fiber laser	Output wavelength 4.3 μm Average power 107 mW Optical efficiency 3.75%	[92]
	As ₂ S ₃	2014	Université Laval	2.8 mm length 98% reflectivity	3.005 μm Er: ZBLAN	Output wavelength 3.77 μm Average power 112 mW Optical efficiency 8.3%	[93]
	As ₂ Se ₃	2019	Ningbo University	1.05–1.23 mm length 97.8–98% reflectivity	3.92 μm Ho ³⁺ :InF ₃	Output wavelength 4.327 μm Average power 0.269 mW Optical efficiency 17.9%	[94]
	Dy ³⁺ :GGSS	2019	Chinese Academy of Sciences	120 mm length Dy ³⁺ :0.3 wt% 125:60:11 /125:66:11.5 core/cladding	1.7 μm Tm ³⁺ :fiber laser	Output wavelength 4.21 μm Impurity absorption peaks 2.4 dB/m $\sigma_e \times \tau_{\text{mea}} 2.62 \times 10^{-23} \text{ cm}^2$ Lifetime 4.61 ms	[95]
Chalcogenide	Tb ³⁺ :GGS	2020	Russian Academy of Sciences	12 mm diameter 56 mm length $2 \times 10^{19} \text{ cm}^{-3}$	2.93 μm Er:YAG laser	Output wavelength 4.9–5.5 μm $\sigma_e(\lambda) = 5 \times 10^{-21} \text{ cm}^2$ Average power 25 mW Lifetime 10 ms	[96]
	Ce ³⁺ :GSGS	2021	Russian Academy of Sciences	12 mm diameter 24 mm length $3 \times 10^{19} \text{ cm}^{-3}$	4.08 μm Fe:ZnSe laser	Output wavelength 5 μm Energy output 0.5 mJ Impurity absorption $6 \times 10^{-3} \text{ cm}^{-1}$ Lifetime 3.7 ms	[97]
	Ce ³⁺ :GSGS	2021	University of Duisburg-Essen	12 mm diameter 24 mm length $3 \times 10^{19} \text{ cm}^{-3}$	4.1 μm Fe:ZnSe laser	Output wavelength 5.2 μm Energy output 35 mJ Optical efficiency 21%	[98]
	Ce ³⁺ :GAGS	2021	University of Nottingham	9 μm diameter 64 mm length 500 ppmw	4.15 μm quantum cascade laser	Output wavelength 4.63 μm Impurity absorption peaks 2.16 dB/m ⁻¹ Lifetime 3.6 ms	[99]
	Pr ³⁺ :GGS	2021	Institute of Chemistry of High-Purity Substances	12 mm diameter 5 mm length $1 \times 10^{20} \text{ cm}^{-3}$	1.54 μm Er:glass laser	Output wavelength 5.5 μm Average power 20 mW Lifetime 3 ms	[100]
		2015	University of Arizona	1 mm length 10–20% reflectivity	2.8 μm Er: ZBLAN	Output wavelength 3.16 μm Average power 7.42 W Optical efficiency 7.55%	[94]
		2017	Hefei University of Technology	0.3 mm length 90% reflectivity	2 μm fiber laser	Output wavelength 3.64 μm Average power 45.2 W Optical efficiency 45.2%	[101]
Tellurite	TBZN	2018	National University of Defense Technology	5.5 mm length 45% reflectivity	2 μm Tm ³⁺ :fiber laser	Output wavelength 3.61 μm Average power 16 W Optical efficiency 45.2%	[102]
		2021	University of Electronic Science and Technology of China	0.2 mm length 69% reflectivity	1.96 μm Tm ³⁺ :fiber laser	Output wavelength 5 μm Average power 52.44 mW Optical efficiency 19%	[103]

From the current research progress, the soft glass fiber (fluoride, chalcogenide and telluride) has low loss in the mid-infrared band. The manufacturing process is relatively mature. Therefore, achieving mid-infrared laser with fiber has been extensively studied by scholars. Among the soft glass fibers, the manufacturing process of ZBLAN fiber

is relatively mature. However, the realization of mid-infrared laser output with high conversion efficiency and the output energy still needs further development; due to the limited manufacturing process of InF_3 and the telluride, there are still difficulties in general commercial use; chalcogenide glass has excellent transmission performance in the mid-infrared band due to its low material dispersion, so it has an indispensable application value at 3–5 μm . For the future, it is necessary to optimize the gain fiber, to increase the pump power and to achieve a higher power mid-infrared laser output.

5. Conclusions

In the past 20 years, based on the progress of new laser materials, optical technology and the traction of application requirements in many fields, the research of mid-infrared laser has made many breakthroughs and rapid progress. In order to improve the performance of mid-infrared lasers, it is urgent to study and improve the physical and chemical properties of the gain medium for achieving mid-infrared laser output and develop technologies to improve the performance of mid-infrared lasers. In general, the paper briefly introduces the development of mid-infrared optical parametric oscillators, direct-pumped mid-infrared solid-state lasers and direct lasing mid-infrared fiber lasers. Looking forward to the future, the main development trends mainly include: (1) output power increases; in the future, we can continue to improve mid-infrared laser technology and soft glass pretreatment and find new gain media to continuously increase the output power of 3–5 μm mid-infrared laser and (2) lift the conversion efficiency furthermore; with the low-loss beam-coupling technology development and the successful development of lower loss optical fiber, based on the improvement of passive InF_3 fiber and chalcogenide purification technology, it can be expected that there is still room for improvement in conversion efficiency.

We can expect that, in the near future, with the continuous improvement of various technologies, the high-power, large-energy mid-infrared laser of 3–5 μm will move from experimental research to practical applications which will play a unique role in scientific research and production.

Author Contributions: Writing—original draft preparation and writing—review and editing, T.R.; methodology, C.W.; funding acquisition, Y.Y.; supervision, F.C., T.D. and Q.P. All authors have read and agreed to the published version of the manuscript.

Funding: Science and Technology Department of Jilin Province in China (Grant No. 202002041JC).

Acknowledgments: We thank the Key Laboratory of Jilin Province Solid-State Laser Technology and Application for the use of the equipment.

Conflicts of Interest: The authors declare no conflict of interest.

References

1. Hu, Z.; Zhu, L.; Di, J.; Cao, X.; Zhou, W. Development of Mid-Infrared Solid Laser Doped with ZnSe as Matrix Material. *Technol. Dev. Chem. Ind.* **2020**, *49*, 36–42.
2. Peng, Y.; Jiang, B.; Fan, J.; Yuan, X.; Zhang, L. Review of Mid-Infrared Laser Materials Directly Pumped by Laser-Diode. *Laser Optoelectron. Prog.* **2015**, *52*, 7–27.
3. Qin, X. *Studies on the Mid-Infrared Optical Parametric Oscillator*; Zhejiang University: Hangzhou, China, 2015.
4. Wang, K.; Pei, B. Mid-infrared Parametric Oscillator with 3.76 μm Output. *Chin. J. Lasers* **2000**, *8*, 691–693.
5. Yao, B.; Wang, Y.; Liu, Q.; Wang, Q. Comparison of LiNbO_3 with KTP optical parametric oscillator operating in mid-infrared spectrum. *J. Harbin Inst. Technol.* **2003**, *10*, 1228–1231.
6. Gang, R. *Studies on the Mid-Infrared Optical Parametric Oscillators and Their Applications*; Sichuan University: Chengdu, China, 2006.
7. Ruebel, F.; Anstett, G.; L'huillier, J.A. Synchronously pumped mid-infrared optical parametric oscillator with an output power exceeding 1 W at 4.5 μm . *Appl. Phys. B Lasers Opt.* **2011**, *102*, 751–755. [[CrossRef](#)]
8. Sheng, Q.; Ding, X.; Shi, C.; Yin, S.; Li, B.; Shang, C.; Yu, X.; Wen, W.; Yao, J. Continuous-wave Mid-infrared Intra-cavity Singly Resonant PPLN—PO Under 880 nm In-band Pumping. *Opt. Express* **2012**, *20*, 8041–8046. [[CrossRef](#)] [[PubMed](#)]
9. Li, H.S.; Liu, Z.Z.; Zheng, J. High Power Mid-infrared MgO:PPLN Optical Parametric Oscillator. *Opt. Optoelectron. Technol.* **2015**, *13*, 64–67.
10. Parsa, S.; Kumar, S.C.; Nandy, B.; Ebrahim-Zadeh, M. Yb-fiber-pumped, High-beam-quality, Idler-resonant Mid-infrared Picosecond Optical Parametric Oscillator. *Opt. Express* **2019**, *27*, 25436–25444. [[CrossRef](#)]

11. Wang, Y.; Ju, Y.; Yao, B. Low-threshold Mid-infrared MgO:PPLN Optical Parametric Generation with High Reflectivity Mirror for Signal Wavelength. *Chin. Opt. Lett.* **2008**, *6*, 204–206.
12. Peng, Y.; Lu, Y.; Xie, G.; Wang, W.; Wu, D. Investigation of Quasi-Phase-Matched Optical Parametric Oscillator Based on PPMgLN. *Chin. J. Lasers* **2008**, *5*, 670–674. [[CrossRef](#)]
13. Liu, J.; Liu, Q.; Yan, X.; Chen, H.; Gong, M. High repetition frequency PPMgOLN mid-infrared optical parametric oscillator. *Laser Phys. Lett.* **2010**, *7*, 630–633. [[CrossRef](#)]
14. Lin, D.; Alam, S.U.; Shen, Y.; Chen, T.; Richardson, D.J. An All-fibre PM MOPA pumped high-power OPO at 3.82 μm based on large aperture PPMgLN. *Proc. Spie Int. Soc. Opt. Eng.* **2012**, *8237*, 82371.
15. Yu, Y.; Chen, X.; Zhao, J.; Wang, C.; Wu, C.; Jin, G. High-repetition-rate Tunable Mid-infrared Optical Parametric Oscillator Based on MgO: Periodically Poled Lithium Niobate. *Opt. Eng.* **2014**, *53*, 61604. [[CrossRef](#)]
16. Chen, T. *Investigation on the Advanced Quasi-Phase-Matching Optical Parametric Oscillators*; Zhejiang University: Hangzhou, China, 2014.
17. Rigaud, P.; Van de Walle, A.; Hanna, M.; Forget, N.; Guichard, F.; Zaouter, Y.; Guesmi, K.; Druon, F.; Georges, P. Supercontinuum—Seeded Few-cycle Mid-infrared Opcpa System. *Opt. Express* **2016**, *24*, 26494–26502. [[CrossRef](#)] [[PubMed](#)]
18. Murray, R.; Runcorn, T.; Guha, S.; Taylor, J.R. High average power parametric wavelength conversion at 331–348 μm in MgO:PPLN. *Opt. Express* **2017**, *25*, 6421–6430. [[CrossRef](#)]
19. Xing, S.; Yu, Y.-j.; Wang, Y.-h.; Fan, H.-r.; Jin, G.-y. Wide Tunable Continuous—Wave Mid Infrared Intro-cavity Optical Parametric Oscillator Based on Multi—Period MgO:PPLN. *ACTA Photonica Sin.* **2018**, *47*, 15–23.
20. Niu, S.; Aierken, P.; Ababaike, M.; Wang, S.; Yusufu, T. Widely tunable, high-energy, mid-infrared (2.2–4.8 μm) laser based on a multi—Grating MgO:PPLN optical parametric oscillator. *Infrared Phys. Technol.* **2020**, *104*, 103121. [[CrossRef](#)]
21. Guo, L.; Yang, Y.; Zhao, S.; Li, T.; Qiao, W.; Ma, B.; Nie, H.; Ye, S.; Wang, R.; Zhang, B.; et al. Room temperature watt-level 3.87 μm MgO:PPLN optical parametric oscillator under pumping with a Tm:YAP laser. *Opt. Express* **2020**, *28*, 32916–32924. [[CrossRef](#)] [[PubMed](#)]
22. Chen, B.Y.; Wang, Y.H.; Yu, Y.J.; Jin, G.Y. High efficiency mid-infrared 3.8 μm MgO:PPLN optical parametric oscillator pumped by narrow linewidth 1064 nm fiber laser. *Chin. Opt.* **2021**, *14*, 361–367.
23. Wang, F.; Nie, H.; Liu, J.; Yang, K.; Zhang, B.; He, J. Miniaturized Widely Tunable MgO:PPLN Nanosecond Optical Parametric Oscillator. *Chin. J. Lasers* **2021**, *5*, 207–215.
24. Baravets, Y.; Honzatko, P.; Todorov, F.; Gladkov, P. Narrowband Widely Tunable Cw Mid-infrared Generator Based on Difference Frequency Generation in Periodically Poled KTP and KTA Crystals. *Opt. Quantum Electron.* **2016**, *48*, 1–6. [[CrossRef](#)]
25. Heiner, Z.; Petrov, V.; Steinmeyer, G.; Vrakking, M.J.J.; Mero, M. 100-kHz, dual-beam OPA delivering high-quality, 5-cycle angular-dispersion-compensated mid-infrared idler pulses at 31 μm . *Opt. Express* **2018**, *26*, 25793–25804. [[CrossRef](#)] [[PubMed](#)]
26. Meng, X.; Wang, Z.; Tian, W.; Song, J.; Wang, X.; Zhu, J.; Wei, Z. High average power 200 fs mid-infrared KTP optical parametric oscillator tunable from 2.61 to 3.84 μm . *Appl. Phys. A* **2021**, *127*, 1–6. [[CrossRef](#)]
27. Sun, Q.; Liu, H.; Huang, N.; Ruan, C.; Zhu, S.; Zhao, W. High efficiency mid-infrared KTA extracavity optical parametric oscillator. *Infrared Laser Eng.* **2010**, *8*, 93–97.
28. Zhang, W.; Wan, Y.; Chen, H.; Wu, Z. Experimental study on mid-infrared KTA optical parametric oscillator. *Laser Infrared* **2011**, *41*, 742–746.
29. Feng, Z.; Duan, Y.; Li, Z.; Wang, H.; Zheng, C.; Zhang, Y.; Zhang, G.; Zhu, H. LD end-pumped Nd:YLF/KTA continuous-wave optical parameter oscillator. *High Power Laser Part. Beams* **2013**, *25*, 1341–1344. [[CrossRef](#)]
30. Liu, Q.; Liu, J.; Zhang, Z.; Gong, M. A high energy 3.75 μm KTA optical parametric oscillator at a critical angle. *Laser Phys. Lett.* **2013**, *10*, 075407. [[CrossRef](#)]
31. Chen, Y.; Li, Y.; Li, W.; Guo, X.; Leng, Y. Generation of High Beam Quality, High-energy and Broadband Tunable Mid-infrared Pulse From a KTA Optical Parametric Amplifier. *Opt. Commun.* **2016**, *365*, 7–13. [[CrossRef](#)]
32. Meng, X.; Wang, Z.; Tian, W.; He, H.; Fang, S.; Wei, Z. Watt-level widely tunable femtosecond mid-infrared KTiOAsO₄ optical parametric oscillator pumped by a 103 μm Yb:KGW laser. *Opt. Lett.* **2018**, *43*, 943–946. [[CrossRef](#)]
33. Cole, B.; Goldberg, L.; Nettleton, J.; Zawilski, K.T.; Pomeranz, L.A.; Schunemann, P.G.; McCarthy, J.C. Compact 12 mJ Mid-ir Pulsed Source Using an Intracavity Kta Opo Followed By a Csp Opa [C]//Solid State Lasers Xxix: Technology and Devices. *Int. Soc. Opt. Photonics* **2020**, *11259*, 1125907.
34. Meng, J.; Cong, Z.; Zhao, Z. 100 Hz High-Energy KTA Dual-Wavelength Optical Parametric Oscillator. *Chin. J. Lasers* **2021**, *48*, 1201009.
35. Bhar, G.C.; Kumbhakar, P.; Satyanarayana, D.V.; Banerjee, N.S.; Nundy, U.; Chao, C.G. Third harmonic generation of CO₂ laser radiation in AgGaSe₂ crystal. *Pramana* **2000**, *55*, 405–412. [[CrossRef](#)]
36. Li, D.; Yang, G.; Xie, Y.; Meng, F.; Guo, J. Experiments of second harmonic generation of 9.3 μm pulsed CO₂ lasers. *Opt. Precis. Eng.* **2009**, *17*, 2684–2691.
37. Yao, Z.; Wang, X.; Xiao, X.; Lu, Y. Third-harmonic generation in AgGaSe₂ crystals based on CO₂ laser. *Laser Technol.* **2013**, *37*, 503–505.
38. Fan, Y.X.; Eckardt, R.C.; Byer, R.L.; Route, R.K.; Feigelson, R.S. AgGaSe₂ Infrared Parametric Oscillator. *Appl. Phys. Lett.* **1984**, *45*, 313–315. [[CrossRef](#)]

39. Boon, P.P.; Fen, W.R.; Chong, C.T.; Xi, X.B. Nanosecond AgGaS₂ optical parametric oscillator with more than 4 micron output. *Jpn. J. Appl. Phys.* **1997**, *36*, L1661. [[CrossRef](#)]
40. Vodopyanov, K.L.; Maffettone, J.P.; Zwieback, I.; Ruderman, W. AgGaS₂ optical parametric oscillator continuously tunable from 3.9 to 11.3 μm. *Appl. Phys. Lett.* **1999**, *75*, 1204–1206. [[CrossRef](#)]
41. Wang, T.J.; Kang, Z.H.; Zhang, H.Z.; He, Q.Y.; Qu, Y.; Feng, Z.S.; Jiang, Y.; Gao, J.Y.; Andreev, Y.M.; Lanskii, G.V. Wide-tunable, High-energy AgGaS₂ Optical Parametric Oscillator. *Opt. Express* **2006**, *14*, 13001–13006. [[CrossRef](#)]
42. Lippert, E.; Fonnum, H.; Arisholm, G.; Stenersen, K. A 22-watt Mid-infrared Optical Parametric Oscillator with V-shaped 3-mirror Ring Resonator. *Opt. Express* **2010**, *18*, 26475–26483. [[CrossRef](#)] [[PubMed](#)]
43. Peng, Y.; Wei, X.; Wang, W. Mid-infrared Optical Parametric Oscillator Based on ZnGeP₂ Pumped by 2 μm laser. *Chin. Opt. Lett.* **2011**, *9*, 71–73.
44. Hemming, A.; Richards, J.; Davidson, A.; Carmody, N.; Bennetts, S.; Simakov, N.; Haub, J. 99 W mid-IR operation of a ZGP OPO at 25% Duty Cycle. *Opt. Express* **2013**, *21*, 10062–10069. [[CrossRef](#)]
45. Gebhardt, M.; Gaida, C.; Kadwani, P.; Sincore, A.; Gehlich, N.; Jeon, C.; Shah, L.; Richardson, M. High Peak-power Mid-infrared ZnGeP₂ Optical Parametric Oscillator Pumped By a Tm: fiber Master Oscillator Power Amplifier System. *Opt. Lett.* **2014**, *39*, 1212–1215. [[CrossRef](#)] [[PubMed](#)]
46. Yao, B.Q.; Shen, Y.J.; Duan, X.M.; Dai, T.Y.; Ju, Y.L.; Wang, Y.Z. A 41 W ZnGeP₂ Optical Parametric Oscillator Pumped By a Q-switched Ho:YAG Laser. *Opt. Lett.* **2014**, *39*, 6589–6592. [[CrossRef](#)] [[PubMed](#)]
47. Han, L.; Yuan, L.; Chen, G.; Hou, T.; Wei, L. 26 W Mid-Infrared Solid-State Laser. *Chin. J. Lasers* **2015**, *42*, 29–34.
48. Eichhorn, M.; Schellhorn, M.; Haakestad, M.W.; Fonnum, H.; Lippert, E. High-pulse-energy mid-infrared fractional-image-rotation-enhancement ZnGeP₂ optical parametric oscillator. *Opt. Lett.* **2016**, *41*, 2596. [[CrossRef](#)] [[PubMed](#)]
49. Wang, L.; Xing, T.; Hu, S.; Wu, X.; Wu, H.; Wang, J.; Jiang, H. Mid-infrared ZGP-OPO with a high optical-to-optical conversion efficiency of 757%. *Opt. Express* **2017**, *25*, 3373–3380. [[CrossRef](#)]
50. Duan, X.M.; Chen, C.; Ding, Y.; Yao, B.Q.; Wang, Y.Z. Widely Tunable Middle Infrared Optical Parametric Oscillator Pumped By the Q-switched Ho:GdVO₄ Laser. *Chin. Phys. Lett.* **2018**, *35*, 54205. [[CrossRef](#)]
51. Qian, C. *Research On The High Power HO:YAG Laser and Its Application to Pump the Mid-And Long-Wave Infrared Laser*; Harbin Institute of Technology: Harbin, China, 2019.
52. Liu, J. *Study on All Solid-State High Beam Quality Mid-Infrared ZnGeP₂ Optical Parametric Oscillator*; Changchun University of Science and Technology: Changchun, China, 2019.
53. Medina, M.A.; Piotrowski, M.; Schellhorn, M.; Wagner, F.R.; Berrou, A.; Hildenbrand-Dhollande, A. Beam Quality and Efficiency of Ns-pulsed High-power Mid-ir Zgp Opos Compared in Linear and Non-planar Ring Resonators. *Opt. Express* **2021**, *29*, 21727–21737. [[CrossRef](#)]
54. Wang, F.; Li, J.; Sun, X.; Yan, B.; Nie, H.; Li, X.; Yang, K.; Zhang, B.; He, J. High-power and high-efficiency 4.3 μm ZGP-OPO. *Chin. Opt. Lett.* **2022**, *20*, 011403. [[CrossRef](#)]
55. Xu, F.; Pan, Q.; Chen, F.; Zhang, K.; Yu, D.; He, Y.; Sun, J. Development progress of Fe²⁺: ZnSe lasers. *Chin. Opt.* **2021**, *14*, 458–469.
56. Yan, C. *Experimental Studies on Cr: ZnSe Laser Pumped By 2 μm Lasers*; Harbin Institute of Technology: Harbin, China, 2008.
57. Myoung, N.; Martyshkin, D.V.; Fedorov, V.V.; Mirov, S.B. Energy Scaling of 4.3 μm Room Temperature Fe: ZnSe Laser. *Opt. Lett.* **2011**, *36*, 6–94. [[CrossRef](#)]
58. Evans, J.W.; Berry, P.A.; Schepler, K.L. 840 mW Continuous-wave Fe:ZnSe Laser Operating at 4140 nm. *Opt. Lett.* **2012**, *37*, 5021–5023. [[CrossRef](#)] [[PubMed](#)]
59. Frolov, M.P.; Korostelin, Y.V.; Kozlovsky, V.I.; Mislavskii, V.V.; Podmar'kov, Y.P.; Savinova, S.A.; Skasyrsky, Y.K. Study of a 2 J pulsed Fe:ZnSe 4 μm laser. *Laser Phys. Lett.* **2013**, *10*, 5001. [[CrossRef](#)]
60. Lancaster, A.; Cook, G.; McDaniel, S.A.; Evans, J.; Berry, P.A.; Shephard, J.D.; Kar, A.K. Mid-infrared Laser Emission from Fe: ZnSe Cladding Waveguides. *Appl. Phys. Lett.* **2015**, *107*, 885–895. [[CrossRef](#)]
61. Mirov, S.; Fedorov, V.; Martyshkin, D.; Moskalev, I.; Mirov, M.; Vasilyev, S. High Average Power Fe:ZnSe and Cr:ZnSe Mid-IR Solid State Lasers. In *Advanced Solid State Lasers*; Optical Society of America: Washington, DC, USA, 2015.
62. Velikanov, S.D.; Gavrishchuk, E.M.; Zaretsky, N.A.; Zakhryapa, A.V.; Ikonnikov, V.B.; Kazantsev, S.Y.; Kononov, I.G.; Maneshkin, A.A.; Mashkovskii, D.A.; Saltykov, E.V.; et al. Repetitively Pulsed Fe: ZnSe Laser with an Average Output Power of 20 W at Room Temperature of the Polycrystalline Active Element. *Quantum Electron.* **2017**, *47*, 303. [[CrossRef](#)]
63. Frolov, M.P.; Korostelin, Y.V.; Kozlovsky, V.I.; Podmar'kov, Y.P.; Skasyrsky, Y.K. High-energy Thermoelectrically Cooled Fe: ZnSe Laser Tunable Over 375–482 μm. *Opt. Lett.* **2018**, *43*, 623–626. [[CrossRef](#)]
64. Frolov, M.P.; Korostelin, Y.V.; Kozlovsky, V.I.; Skasyrsky, Y.K. Study of a Room Temperature, Monocrystalline Fe: ZnSe Laser, Pumped By a High-energy, Free-running Er: Yag Laser. *Laser Phys.* **2019**, *29*, 85004. [[CrossRef](#)]
65. Li, Y.Y.; Ju, Y.L.; Dai, T.Y.; Duan, X.M.; Guo, C.F.; Xu, L.W. A Gain-switched Fe: ZnSe Laser Pumped By a Pulsed Ho, Pr: LFF Laser. *Chin. Physlett.* **2019**, *36*, 24–26.
66. Li, Y.Y.; Dai, T.Y.; Duan, X.M.; Guo, C.F.; Xu, L.W.; Ju, Y.L. Fe:znse Laser Pumped By a 2.93 μm Cr, Er:yag Laser. *Chin. Phys. B* **2019**, *28*, 195–198.
67. Uehara, H.; Tsunai, T.; Han, B.; Goya, K.; Yasuhara, R.; Potemkin, F.; Kawanaka, J.; Tokita, S. 40 kHz, 20 ns acousto-optically Q-switched 4 μm Fe: ZnSe laser pumped by fluoride fiber laser. *Opt. Lett.* **2020**, *45*, 2788–2791. [[CrossRef](#)]

68. Pushkin, A.V.; Migal, E.A.; Tokita, S.; Korostelin, Y.V.; Potemkin, F.V. Femtosecond graphene mode-locked Fe:ZnSe laser at 4.4 μm . *Opt. Lett.* **2020**, *45*, 738–741. [[CrossRef](#)] [[PubMed](#)]
69. Pan, Q.; Xie, J.; Chen, F.; Zhang, K.; Yu, D.; He, Y.; Sun, J. Transversal Parasitic Oscillation Suppression in High Gain Pulsed Fe²⁺: ZnSe Laser at Room Temperature. *Opt. Laser Technol.* **2020**, *127*, 106151. [[CrossRef](#)]
70. Martyshkin, D.; Karki, K.; Fedorov, V.; Mirov, S. Room temperature, nanosecond, 60 mJ/pulse Fe: ZnSe master oscillator power amplifier system operating over 3.8–5.0 μm . *Opt. Express* **2020**, *29*, 2387–2393. [[CrossRef](#)]
71. Demirbas, U.; Sennaroglu, A. Intracavity—pumped Cr²⁺: ZnSe laser with ultrabroad tuning range between 1880 and 3100 nm. *Opt. Lett.* **2006**, *31*, 2293–2295. [[CrossRef](#)]
72. Moskalev, I.S.; Fedorov, V.V.; Mirov, S.B. High-power Single-frequency Tunable Cw Er-fiber Laser Pumped Cr²⁺: ZnSe Laser. *Proc. Spie Int. Soc. Opt. Eng.* **2007**, *6552*, 655210.
73. Sorokin, E.; Sorokina, I.T.; Mirov, M.S.; Fedorov, V.V.; Moskalev, I.S.; Mirov, S.B. Ultrabroad Continuous-Wave Tuning of Ceramic Cr: ZnSe and Cr: ZnS Lasers. In *Advanced Solid-State Photonics 2010 Advanced Solid-State Photonics 2010*; Optical Society of America: Washington, DC, USA, 2010.
74. Aikawa, S.; Yumoto, M.; Saitoh, T.; Wada, S. Mid-infrared Tunable Pulsed Laser Based on Cr²⁺ doped Ii–vi Chalcogenide. *J. Cryst. Growth* **2021**, *575*, 126341. [[CrossRef](#)]
75. Li, W.W.; Zhang, X.J.; Wang, H. Research Progress of Mid-Infrared Rare Earth Ion—Doped Fiber Lasers at 3 μm . *Laser Optoelectron. Prog.* **2019**, *56*, 170605. [[CrossRef](#)]
76. Sujecki, S. Modelling and Design of Lanthanide Ion-doped Chalcogenide Fiber Lasers: Progress Towards the Practical Realization of the First Mir Chalcogenide Fiber Laser. *Fibers* **2018**, *6*, 25. [[CrossRef](#)]
77. Henderson-Sapir, O.; Munch, J.; Ottaway, D.J. Mid-infrared fiber lasers at and beyond 35 μm using dual-wavelength pumping. *Opt. Lett.* **2014**, *39*, 493–496. [[CrossRef](#)]
78. Shen, Y.; Wang, Y.; Luan, K.; Huang, K.; Tao, M.; Chen, H.; Yi, A.; Feng, G.; Si, J. Watt-level Passively Q-switched Heavily Er³⁺: ZBLAN Fiber Laser with a Semiconductor Saturable Absorber Mirror. *Sci. Rep.* **2016**, *6*, 26659. [[CrossRef](#)]
79. Qin, Z.; Hai, T.; Xie, G.; Ma, J.; Yuan, P.; Qian, L.; Li, L.; Zhao, L.; Shen, D. Black Phosphorus Q-switched and Mode-locked Mid-infrared Er: ZBLAN Fiber Laser at 3.5 μm Wavelength. *Opt. Express* **2018**, *26*, 8224. [[CrossRef](#)]
80. Maes, F.; Stihler, C.; Pleau, L.P.; Fortin, V.; Limpert, J.; Bernier, M.; Vallée, R. 3.42 μm lasing in heavily-erbium-doped fluoride fibers. *Opt. Express* **2019**, *27*, 2170–2183. [[CrossRef](#)]
81. Yang, J.; Luo, H.; Liu, F.; Li, J.; Liu, Y. Widely Tunable Gain-switched Er³⁺ doped ZrF₄ Fiber Laser from 3.4 to 3.7 μm . *IEEE Photonics Technol. Lett.* **2020**, *32*, 1335–1338. [[CrossRef](#)]
82. Fang, Z.; Zhang, C.; Liu, J.; Chen, Y.; Fan, D. 3.46 μm Q-switched Er³⁺: Zblan Fiber Laser Based on a Semiconductor Saturable Absorber Mirror. *Opt. Laser Technol.* **2021**, *141*, 107131. [[CrossRef](#)]
83. Li, J.; Hudson, D.D.; Jackson, S.D. High-power Diode-pumped Fiber Laser Operating at 3 μm . *Opt. Lett.* **2011**, *36*, 3642–3644. [[CrossRef](#)] [[PubMed](#)]
84. Li, J.; Hu, T.; Jackson, S.D. Dual Wavelength Q-switched Cascade Laser. *Opt. Lett.* **2012**, *37*, 2208–2210. [[CrossRef](#)] [[PubMed](#)]
85. Zhu, G.; Zhu, X.; Balakrishnan, K.; Norwood, R.A.; Peyghambarian, N. Fe²⁺: Znse and Graphene Q-switched Singly Ho³⁺: ZBLAN Fiber Lasers at 3 μm . *Opt. Mater. Express* **2013**, *3*, 1365–1377. [[CrossRef](#)]
86. Maes, F.; Fortin, V.; Poulain, S.; Poulain, M.; Carrée, J.-Y.; Bernier, M.; Vallée, R. Room-temperature fiber laser at 392 μm . *Optics* **2018**, *5*, 761–764. [[CrossRef](#)]
87. Zhou, F. *Fundamental Research on Ho³⁺ and Dy³⁺ doped Fluoride Fiber Lasers in 4 μm Band*; University of Electronic Science and Technology of China: Chengdu, China, 2021.
88. Majewski, M.R.; Jackson, S.D. Highly Efficient Mid-infrared Dysprosium Fiber Laser. *Opt. Lett.* **2016**, *41*, 2173. [[CrossRef](#)] [[PubMed](#)]
89. Majewski, M.R.; Woodward, R.I.; Jackson, S.D. Dysprosium-doped ZBLAN fiber laser tunable from 2.8 μm to 3.4 μm , pumped at 1.7 μm . *Opt. Lett.* **2018**, *43*, 971. [[CrossRef](#)] [[PubMed](#)]
90. Fortin, V.; Jobin, F.; LaRose, M.; Bernier, M.; Vallée, R. 10-W-level monolithic dysprosium-doped fiber laser at 324 μm . *Opt. Lett.* **2019**, *44*, 491–494. [[CrossRef](#)]
91. Jobin, F.; Paradis, P.; Fortin, V.; Magnan-Saucier, S.; Bernier, M.; Vallée, R. 1.4 W In-band Pumped Dy³⁺ doped Gain-switched Fiber Laser at 3.24 μm . *Opt. Lett.* **2020**, *45*, 5028–5031. [[CrossRef](#)]
92. Bernier, M.; Fortin, V.; El-Amraoui, M.; Messaddeq, Y.; Vallée, R. 3.77 μm Fiber Laser Based on Cascaded Raman Gain in a Chalcogenide Glass Fiber. *Opt. Lett.* **2014**, *39*, 2052–2055. [[CrossRef](#)] [[PubMed](#)]
93. Peng, X.; Zhang, P.; Wang, X.; Guo, H.; Wang, P.; Dai, S. Modeling and Simulation of a Mid-ir 4.3 μm Raman Laser in Chalcogenide Glass Fibers. *OSA Contin.* **2019**, *2*, 2281–2292. [[CrossRef](#)]
94. Zhu, G.; Geng, L.; Zhu, X.; Li, L.; Chen, Q.; Norwood, R.A.; Manzur, T.; Peyghambarian, N. Towards Ten-watt-level 3–5 μm Raman Lasers Using Tellurite Fiber. *Opt. Express* **2015**, *23*, 7559. [[CrossRef](#)]
95. Xiao, X.; Xu, Y.; Cui, J.; Liu, X.; Cui, X.; Wang, X.; Dai, S.; Guo, H. Structured Active Fiber Fabrication and Characterization of a Chemically High-purified Dy³⁺-doped Chalcogenide Glass. *J. Am. Ceram. Soc.* **2020**, *103*, 2432–2442. [[CrossRef](#)]
96. Churbanov, M.F.; Denker, B.I.; Galagan, B.I.; Koltashev, V.V.; Plotnichenko, V.G.; Sukhanov, M.V.; Sverchkov, S.E.; Velmuzhov, A.P. First Demonstration of ~5 μm Laser Action in Terbium-doped Selenide Glass. *Appl. Phys. B* **2020**, *126*, 1–5. [[CrossRef](#)]

97. Denker, B.I.; Galagan, B.I.; Sverchkov, S.E.; Koltashev, V.V.; Plotnichenko, V.G.; Sukhanov, M.V.; Velmuzhov, A.P.; Frolov, M.P.; Korostelin, Y.V.; Kozlovsky, V.I.; et al. Resonantly Pumped Ce³⁺ Mid-infrared Lasing in Selenide Glass. *Opt. Lett.* **2021**, *46*, 4002–4004. [[CrossRef](#)]
98. Fjodorow, P.; Frolov, M.P.; Leonov, S.O.; Denker, B.I.; Galagan, B.I.; Sverchkov, S.E.; Koltashev, V.V.; Plotnichenko, V.G.; Sukhanov, M.V.; Velmuzhov, A.P. Mid-infrared laser performance of Ce³⁺-doped selenide glass. *Opt. Express* **2021**, *29*, 17. [[CrossRef](#)]
99. Nunes, J.J.; Crane, R.W.; Furniss, D.; Tang, Z.Q.; Mabwa, D.; Xiao, B.; Benson, T.M.; Farries, M.; Kalfagiannis, N.; Barney, E.; et al. Room Temperature Mid-infrared Fiber Lasing Beyond 5 μm in Chalcogenide Glass Small-core Step Index Fiber. *Opt. Lett.* **2021**, *46*, 3504–3507. [[CrossRef](#)]
100. Churbanov, M.F.; Denker, B.I.; Galagan, B.I.; Koltashev, V.V.; Plotnichenko, V.G.; Snopatin, G.E.; Sukhanov, M.V.; Sverchkov, S.E.; Velmuzhov, A.P. Laser Potential of Pr³⁺ Doped Chalcogenide Glass in 5–6 μm Spectral Range. *J. Non-Cryst. Solids* **2021**, *559*, 120592. [[CrossRef](#)]
101. Ni, C.; Gao, W.; Chen, X.; Chen, L.; Zhou, Y.; Zhang, W.; Hu, J.; Liao, M.; Suzuki, T.; Ohishi, Y. Theoretical Investigation on Mid-infrared Cascaded Raman Fiber Laser Based on Tellurite Fiber. *Appl. Opt.* **2017**, *56*, 9171. [[CrossRef](#)] [[PubMed](#)]
102. Yao, T.; Huang, L.; Zhou, P.; Lei, B.; Leng, J.; Chen, J. Power Scaling on Tellurite Glass Raman Fibre Lasers for Mid-infrared Applications. *High Power Laser Sci. Eng.* **2018**, *6*, 79–87. [[CrossRef](#)]
103. Hou, Y.; Wu, X.; Wu, Q.; Liu, F.; Luo, H.; Ouellette, F.; Li, J. Theoretical Investigation of a Multistage Cascaded Fiber Raman Soliton Frequency Shift System in Mid-infrared Region. *IEEE Photonics J.* **2021**, *13*, 1–8. [[CrossRef](#)]